

An *ab initio* investigation of Bi_2Se_3 topological insulator deposited on amorphous SiO_2

I. S. S. de Oliveira*

*Departamento de Física, Universidade Federal de Lavras,
C.P. 3037, 37200-000, Lavras, MG, Brazil*

W. L. Scopel†

*Departamento de Física, Universidade Federal do Espírito Santo, Vitória, ES, 29075-910, Brazil and
Departamento de Ciências Exatas, Universidade Federal Fluminense, Volta Redonda, RJ, 27255-250, Brazil*

R. H. Miwa‡

*Instituto de Física, Universidade Federal de Uberlândia,
C.P. 593, 38400-902, Uberlândia, MG, Brazil*

(Dated: October 12, 2018)

We use first-principles simulations to investigate the topological properties of Bi_2Se_3 thin films deposited on amorphous SiO_2 , $\text{Bi}_2\text{Se}_3/\text{a-SiO}_2$, which is a promising substrate for topological insulator (TI) based device applications. The Bi_2Se_3 films are bonded to a- SiO_2 mediated by van der Waals interactions. Upon interaction with the substrate, the Bi_2Se_3 topological surface and interface states remain present, however the degeneracy between the Dirac-like cones is broken. The energy separation between the two Dirac-like cones increases with the number of Bi_2Se_3 quintuple layers (QLs) deposited on the substrate. Such a degeneracy breaking is caused by (i) charge transfer from the TI to the substrate and charge redistribution along the Bi_2Se_3 QLs, and (ii) by deformation of the QL in contact with the a- SiO_2 substrate. We also investigate the role played by oxygen vacancies (V_{O}) on the a- SiO_2 , which increases the energy splitting between the two Dirac-like cones. Finally, by mapping the electronic structure of $\text{Bi}_2\text{Se}_3/\text{a-SiO}_2$, we found that the a- SiO_2 surface states, even upon the presence of V_{O} , play a minor role on gating the electronic transport properties of Bi_2Se_3 .

I. INTRODUCTION

Three-dimensional (3D) topological insulators (TIs) are a recently discovered class of materials and have attracted great attention due to their unique properties. They are insulators in the bulk phase but present topologically protected metallic states at the surface or interface with a trivial insulator¹. The topological surface states (TSSs) or interface states (TISs) are spin-polarized Dirac fermion states, protected by time-reversal symmetry, and in the absence of magnetic impurities these states are insensitive to backscattering processes induced by time-reversal invariant impurities or defects¹⁻⁶. These properties make TI materials suitable for spintronics applications⁷. In particular, Bi_2Se_3 is one of the most investigated 3D-TI, it has a rhombohedral structure composed by quintuple layers (QLs) of Se and Bi covalently bonded, and these QLs are stacked along the c -axis by van der Waals (vdW) interactions⁸⁻¹⁰.

To take advantage of TIs materials for technological applications is necessary that the topologically protected states remain intact upon interaction with other materials. Thus, the substrate choice for Bi_2Se_3 growth should be such that it preserves the TIs properties. Bi_2Se_3 has been grown on various substrates, e.g., graphene, $\text{Si}(111)$, CaF_2 , CdS , Al_2O_3 , SiO_2 , among others¹¹. Amorphous phases of dielectric or insulator materials are widely used for electronic applications, and an interesting material often used for this purpose is the amorphous SiO_2 (a- SiO_2). Bi_2Se_3 thin films have been grown on a- SiO_2 by

different experimental technics^{12,13}, and it has recently been shown to present topologically protected surface states¹⁴⁻¹⁶.

To better understand the interaction between Bi_2Se_3 thin films and the a- SiO_2 substrate, we perform a first-principles investigation for increasing number of Bi_2Se_3 quintuple layers deposited on a- SiO_2 , $(\text{Bi}_2\text{Se}_3)_n/\text{a-SiO}_2$. We find that the Bi_2Se_3 layers are bonded to the a- SiO_2 surface mediated by vdW interactions; where the lattice structure of the Bi_2Se_3 QLs are preserved. At the interface region we have found a net electronic charge transfer from the bottom-most Bi_2Se_3 QL to the a- SiO_2 surface. There is a down-shift (up-shift) of the metallic TSSs (TISs), promoting electronic transport mediated by electrons (holes) on the surface (interface) Bi_2Se_3 QLs. We have also considered the presence of oxygen vacancies (V_{O}) on the surface, a- $\text{SiO}_2[V_{\text{O}}]$, which is a quite common intrinsic defect. The strength of the $\text{Bi}_2\text{Se}_3 \leftrightarrow \text{a-SiO}_2[V_{\text{O}}]$ interaction is the same as that of $\text{Bi}_2\text{Se}_3/\text{a-SiO}_2$, as well as the maintenance of the Bi_2Se_3 lattice structure. Further electronic structure calculations show that the a- SiO_2 surface states, even upon the presence of V_{O} , play a minor role on gating the electronic transport properties of Bi_2Se_3 ; where the V_{O} defect level is resonant within the valence band of Bi_2Se_3 , lying below the topologically protected metallic states.

II. COMPUTATIONAL DETAILS

The calculations are performed based on the density-functional theory (DFT), as implemented in the Vienna *ab initio* simulation package (VASP)¹⁷. We use the generalized gradient approximation (GGA), in the form proposed by Perdew, Burke and Ernzerhof¹⁸, to describe the exchange-correlation functional. The Kohn-Sham orbitals are expanded in a plane wave basis set with an energy cutoff of 400 eV. The electron-ion interactions are taken into account using the Projector Augmented Wave (PAW) method¹⁹. The Brillouin Zone is sampled according to the Monkhorst-Pack method²⁰, using at least a $2 \times 2 \times 1$ mesh. We have also used a functional that accounts for dispersion effects, representing van der Waals (vdW) forces, according to the method developed by Tkatchenko-Scheffler (TS)²¹, which is implemented on VASP²². The inclusion of van der Waals forces in the simulations is necessary to obtain the correct vdW gap between consecutive QLs²³, the interaction between the a-SiO₂ substrate and Bi₂Se₃ is also better described with the inclusion of vdW interactions.

The amorphous structure was generated through *ab initio* molecular dynamics (MD) simulations based on the DFT approach as implemented in the VASP code. In Ref.²⁴, we present details on the generation procedure of amorphous SiO₂ bulk structure. In order to generate the a-SiO₂ surface, we have considered a a-SiO₂ slab, where the boundary condition perpendicular to the surface plane (z direction) has been removed by introducing a vacuum region of 10 Å. The atomic positions have been relaxed until atomic forces were lower than 25 meV/Å.

III. RESULTS AND DISCUSSION

Our study starts by calculating the energetic stability and the equilibrium geometry of Bi₂Se₃ on the a-SiO₂ substrate, Bi₂Se₃/a-SiO₂. The binding energy (E^b) of Bi₂Se₃/a-SiO₂ is defined as,

$$E^b = E[\text{Bi}_2\text{Se}_3/\text{a-SiO}_2] - E[\text{Bi}_2\text{Se}_3] - E[\text{a-SiO}_2],$$

where $E[\text{Bi}_2\text{Se}_3]$ and $E[\text{a-SiO}_2]$ are the total energies of the separated components: a QL of Bi₂Se₃ and the a-SiO₂ surface; and $E[\text{Bi}_2\text{Se}_3/\text{a-SiO}_2]$ represents the total energy of the final system, a single QL of Bi₂Se₃ adsorbed on the a-SiO₂ surface, as indicated in the inset of Fig. 1. Our results of E^b , as a function of the vertical distance d_z , are presented in Fig. 1. We find $E^b = -8.68 \text{ meV}/\text{Å}^2$, for an (averaged) equilibrium distance of $d_z = 2.90 \text{ Å}$. As observed for the QLs in the Bi₂Se₃ bulk, there is no chemical bonding between the Bi₂Se₃ and the a-SiO₂ substrate, where the Bi₂Se₃ ↔ a-SiO₂ interaction is ruled by vdW forces. Similar picture has been verified for graphene on the a-SiO₂ surface, where we found $E^b = 6.3 \text{ eV}/\text{Å}^2$,²⁵ which is in good agreement with the experimental estimative of Ishigami *et al.*, $6 \text{ meV}/\text{Å}^2$.²⁶

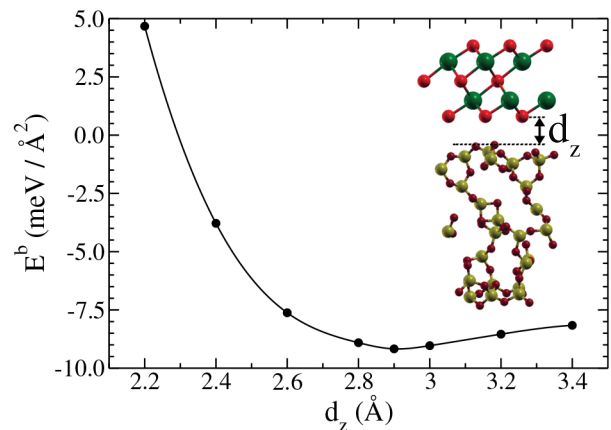


FIG. 1. Binding energy of 1QL-Bi₂Se₃/a-SiO₂ as a function of separation distance along the perpendicular direction (d_z), as represented in the structure shown in the inset. Green (light red) balls represent Bi (Se) atoms, and yellow (dark red) balls represent Si (O) atoms.

The absence of chemical bonding between the Bi₂Se₃ QL and the a-SiO₂ surface has been maintained even upon the presence of oxygen vacancies (V_O) on the a-SiO₂ surface (a-SiO₂[V_O]); V_O is a quite common intrinsic defect in SiO₂. We obtained practically the same values of binding energy, $E^b = -9.00 \text{ meV}/\text{Å}^2$, and an equilibrium distance d_z of 2.96 Å. For both systems, Bi₂Se₃/a-SiO₂ and /a-SiO₂[V_O], the atomic displacements at the interface region are very small, preserving the lattice structure of Bi₂Se₃, supporting recent experimental results of scanning transmission electron microscopy.¹⁵ Further comparisons indicate that, (i) the distance between the substrate and the Bi₂Se₃ QL is approximately 9% larger than the separation distance between consecutive QLs in the Bi₂Se₃ bulk phase,^{23,27} and (ii) the Bi₂Se₃/a-SiO₂ binding energy is about 40% lower (in absolute value) compared with the one between QLs in Bi₂Se₃ bulk phase. That is, the Bi₂Se₃ ↔ Bi₂Se₃ interaction is stronger than that between Bi₂Se₃ and the a-SiO₂ surface.

Next we investigate the electronic and topological properties of Bi₂Se₃/a-SiO₂, as a function of the number of Bi₂Se₃ QLs (n) on the a-SiO₂ surface, (Bi₂Se₃) _{n} /a-SiO₂. In (Bi₂Se₃) _{n} /a-SiO₂, the opposite sides of Bi₂Se₃ are in contact with different environments (with different dielectric constants), *viz.*: one (top-most) is in contact with a vacuum region, and the other (bottom-most) in contact with the a-SiO₂ surface. There is no inversion symmetry in (Bi₂Se₃) _{n} /a-SiO₂, and thus the energy degeneracy between the edge (QL) states can be removed. Indeed this is what we verify in Fig. 2, where we present the electronic band structure of (Bi₂Se₃) _{n} /a-SiO₂ for $n=3, 4, 5, 6$, and 8. The size of blue (red) circles (in Fig. 2) is proportional to the contribution of the Bi- p_z orbitals of the bottom-(top)-most QL of the (Bi₂Se₃) _{n} . We find that the surface states present an energy gap for

$n=3$ and 4, characterized by a Rashba-like band splitting near the Γ point. Those Rashba-like energy bands present similar spatial distribution, and spin-texture (not shown) when compared with the ones observed for thin films of Bi_2Se_3 on $\text{SiC}(0001)$ and $\text{InP}(111)$.^{28,29} In addition, it is worth noting that electronic contributions from the edge QLS to the band apex, indicated by arrows near the Γ point in Fig. 2(a), are reduced for $n=3$ and 4. Those states are delocalized, spreading out along the Bi_2Se_3 layers, as verified for Bi_2Se_3 on $\text{InP}(111)$.²⁹ Such a delocalization is suppressed upon the formation of gapless Dirac bands for $n = 5, 6$ and 8 [Figs.2(c)–2(e)], *i.e.* the topologically protected metallic bands become fully localized on the top-most surface, and bottom-most interface QLS of $(\text{Bi}_2\text{Se}_3)_n/\text{a-SiO}_2$.

As shown in Figs.2(c)–2(e), the topological surface/interface states (TSSs/TISs) move downward/upward with respect to the Fermi level. Those results suggest that there is a local *p*-type (*n*-type) doping of the edge QLS of Bi_2Se_3 . Indeed, based on the Bader charge analysis method,³⁰ with the code developed by the Henkelman's group,³¹ we find a net charge transfer from the bottom-most Bi_2Se_3 QL to the *a*- SiO_2 surface atoms, giving rise to an electrostatic dipole at the interface region, as well as an electronic charge density rearrangement along the Bi_2Se_3 slab. In order to provide a measurement of the charge density imbalance along the Bi_2Se_3 layer, we compare the total charge densities at the edge QLS of $(\text{Bi}_2\text{Se}_3)_n/\text{a-SiO}_2$ with the ones of a free standing $(\text{Bi}_2\text{Se}_3)_n$ film. We find that the charge density reduces by $5.5\text{--}6.0 \times 10^{12} e/\text{cm}^2$ in the bottom-most QL, while it increases by $0.2\text{--}1.0 \times 10^{12} e/\text{cm}^2$ in the top-most QL. Thus, supporting the down-shift (up-shift) of the TSSs (TISs) lying on the surface (interface) QL of $(\text{Bi}_2\text{Se}_3)_n/\text{a-SiO}_2$.

The separation between the Dirac points [V' in Fig. 2(g)] increases almost linearly with the number of QLS, even one QL before the closing of the energy gap, $n=4$. Such a dependence of V' , with the width (d) of $(\text{Bi}_2\text{Se}_3)_n$, can be attributed to the presence of a net electric field (E^{net}) along the $(\text{Bi}_2\text{Se}_3)_n$ film, $V' \propto E^{\text{net}}d$.³² Where E^{net} comes from the charge density imbalance discussed above, and the band bending due to the charge transfer at the $(\text{Bi}_2\text{Se}_3)_n/\text{SiO}_2$ interface. By changing the electronic structure at the $\text{Bi}_2\text{Se}_3/\text{a-SiO}_2$ interface region, we may have different values of V' for a given $(\text{Bi}_2\text{Se}_3)_n$ width; for instance, the presence of oxygen vacancies on the *a*- SiO_2 surface. As shown in Fig. 2(f), V' increases by 37 meV, $V'=47 \rightarrow 84$ meV in $(\text{Bi}_2\text{Se}_3)_8/\text{a-SiO}_2[\text{V}_\text{O}]$.

Tuning the electron chemical potential within the energy window given by V' , the energy separation between the opposite edge states of $\text{Bi}_2\text{Se}_3/\text{a-SiO}_2$ will promote topologically protected electron (hole) currents on the top-most surface (bottom-most interface) states of Bi_2Se_3 . In addition, the up-shift of the interface states in $\text{Bi}_2\text{Se}_3/\text{a-SiO}_2$ indicates that the scattering rate between the TISs and the bulk continuum states will be

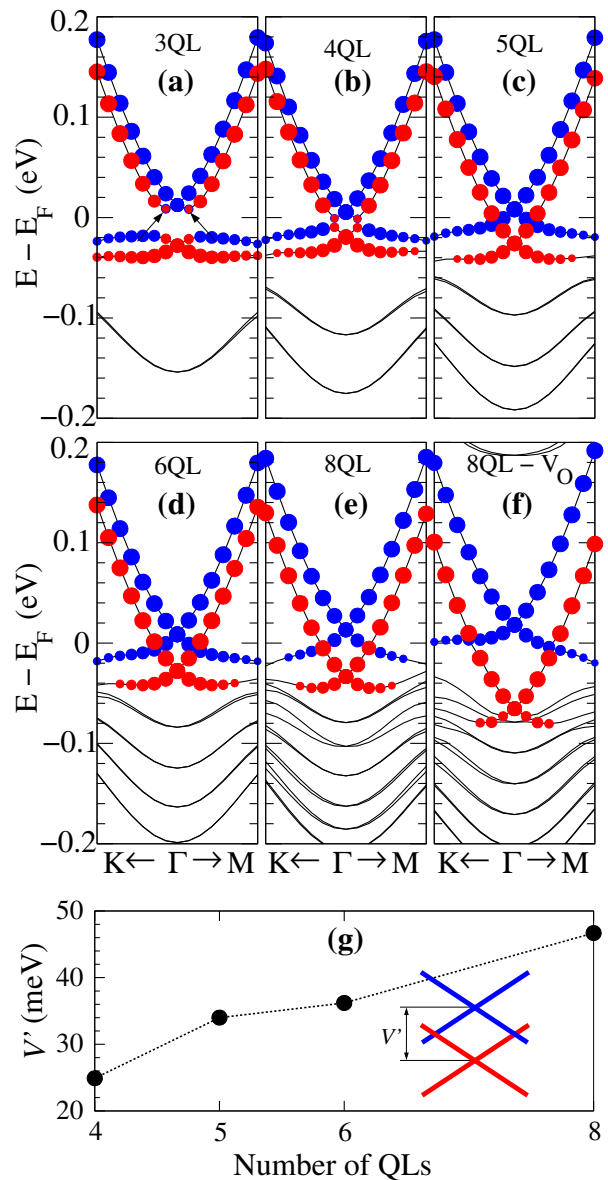


FIG. 2. (a)–(e) Band structures for n QLs- Bi_2Se_3 deposited on *a*- SiO_2 , where n ranges from 3 to 8. Blue circles are contributions of Bi p_z -orbitals from the bottom-most QL (interface with the substrate), and red circles for the top-most QL (vacuum interface). The circles size are proportional to the orbital contribution for each computed k-point. (f) Band structure for $(\text{Bi}_2\text{Se}_3)_8/\text{a-SiO}_2[\text{V}_\text{O}]$. (g) Energy gap at the Γ -point between Dirac-like cones from Bi_2Se_3 topological surface and interface states, as a function of number of QLS deposited on the *a*- SiO_2 substrate.

reduced, while the TSSs will face an increase of such a scattering rate.³³ Further control of the energy positions of those TSSs and TISs can be done by an external electric field. Indeed, top-gate structures has been used to control the topological transport properties in thin films of Bi_2Se_3 on dielectric substrates.^{14,16,34,35}

In Fig. 3(a), we present the energy positions of the

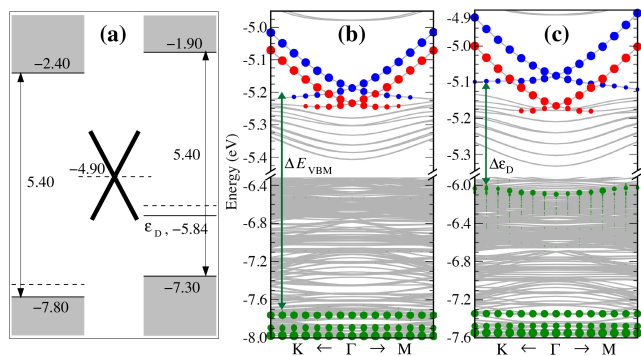


FIG. 3. (a) Valence band maximum and conduction band minimum for a-SiO₂ (left) and a-SiO₂[V_O] (right), dashed black lines represent the Fermi energy, and ϵ_D the O-vacancy defect level. The Dirac cone for a free standing (Bi₂Se₃)₈ film is represented on the figure's center. (b) Band structure of (Bi₂Se₃)₈/a-SiO₂ and (c) (Bi₂Se₃)₈/a-SiO₂[V_O]. Blue (red) circles are Bi p_z-orbitals contribution for the bottom-most (top-most) Bi₂Se₃ QL, and green circles the projection of a-SiO₂ orbitals. All energy values are related to the vacuum energy level ($E_{vac} = 0$).

isolated systems, valence band maximum (VBM) and the conduction band minimum (CBM) of pristine a-SiO₂ (left), and defective a-SiO₂[V_O] (right) surfaces. Here, we have considered the vacuum level as the energy reference. The doubly occupied V_O defect level ($\epsilon_D = -5.84$ eV) lies at 1.46 eV above the valence band maximum.³⁶ In the (Bi₂Se₃)₈ film [Fig. 3(a) (center)], the Fermi level is given by the crossing on the TSSs; it lies in the energy gap of a-SiO₂, and above the defect level (ϵ_D) of a-SiO₂[V_O]. The position of the Fermi energy (E_F), with respect to the vacuum level, corresponds to the work function (Φ_0) of free standing (Bi₂Se₃)₈, $\Phi_0 = 4.90$ eV. Meanwhile, the work function of the final systems (Φ), (Bi₂Se₃)₈/a-SiO₂ and /a-SiO₂[V_O], increases with respect to Φ_0 . Comparing those work functions, $\Delta E_F = \Phi - \Phi_0$, we can infer the band bending of (Bi₂Se₃)₈ upon the formation of the Bi₂Se₃/a-SiO₂ interface.³⁷ We find positive values of ΔE_F , 0.30 and 0.21 eV for (Bi₂Se₃)₈/a-SiO₂ and /a-SiO₂[V_O], respectively, and thus supporting the electron transfer from Bi₂Se₃ to the a-SiO₂ surface.

Aiming the development of electronic devices composed by thin films of Bi₂Se₃ with a-SiO₂ as the dielectric gate, it is important to get a picture of the en-

ergy positions of the TSSs and TISs in Bi₂Se₃/a-SiO₂. In Figs. 3(b) and 3(c) we present the electronic band structures of the final systems, (Bi₂Se₃)₈/a-SiO₂ and /a-SiO₂[V_O], respectively, including the orbital projection to the a-SiO₂ surface. Those energy band diagrams show that (near the Γ point) the TSSs and TISs states lie at about (i) 2.6 eV above the VBM of the a-SiO₂ surface [ΔE_{VBM} in Fig. 3(b)], and (ii) 0.9 eV above the V_O defect level [$\Delta \epsilon_D$ in Fig. 3(c)], which is resonant within the valence band of Bi₂Se₃. Thus, indicating that the electronic states of the a-SiO₂ surface, even upon the presence of intrinsic defects like V_O, will play a minor role on gating the electronic transport properties, mediated by the topological states, for Bi₂Se₃ films.

IV. CONCLUSIONS

We have performed an *ab initio* investigation of Bi₂Se₃ topological insulator deposited on amorphous a-SiO₂ substrate. The Bi₂Se₃ layers are bonded to the a-SiO₂ surface through vdW interactions; preserving the lattice structure of the Bi₂Se₃ QLs. Topologically protected edge states are observed on the surface as well as at the interface layers of Bi₂Se₃, however they are no longer degenerated. The TSSs exhibit an energy-down-shift, followed by the up-shift of the TISs. The degeneracy break is caused by the combination of two effects: (i) charge transfer from the TI to the substrate and charge redistribution along the Bi₂Se₃ QLs, resulting in electron depletion (accumulation) at the closest (furthest) QL from the substrate; and (ii) the Bi₂Se₃ deformation due to the a-SiO₂ interaction. Such an energy separation is increased by the presence of V_O. Finally, by mapping the energy positions of the Bi₂Se₃ edge states, the VBM, CBM, and the V_O defect level of a-SiO₂, we verify that the a-SiO₂ surface states will play a minor role on gating the electronic transport properties in Bi₂Se₃/a-SiO₂ systems.

ACKNOWLEDGMENTS

This work was supported by the Brazilian Nanocarbon Institute of Science and Technology (INCT/Nanocarbono), and the Brazilian agencies CNPq, FAPES and FAPEMIG. The authors also acknowledge the computational support from CENAPAD/SP.

* igor.oliveira@dfi.ufla.br

† wlscofel@if.ufr.br

‡ hiroki@infis.ufu.br

¹ M. Z. Hasan and C. L. Kane, Rev. Mod. Phys. **82**, 3045 (2010).

² L. A. Wray, S. Xu, Y. Xia, D. Hsieh, A. V. Fedorov, Y. S. Hor, R. J. Cava, A. Bansil, H. Lin, and M. Z. Hasan, Nat.

Phys. **7**, 32 (2011).

³ Y. L. Chen, J. Chu, J. G. Analytis, Z. K. Liu, K. Igarashi, H. Kuo, X. L. Qi, S. K. Mo, R. G. Moore, D. H. Lu, M. Hashimoto, T. Sasagawa, S. C. Zhang, I. R. Fisher, Z. Hussain, and Z. X. Shen, Science **329**, 659 (2010).

⁴ S. Y. Xu, M. Neupane, C. Liu, D. Zhang, A. Richardella, L. A. Wray, N. Alidoust, M. Leandersson, T. Balasubrama-

- nian, J. Sánchez-Barriga, O. Rade, G. Landolt, B. Slomski, J. H. Dil, J. Osterwalder, T. R. Chang, H. T. Jeng, H. Lin, A. Basil, N. Samarth, and M. Z. Hasan, *Nature Phys.* **8**, 616 (2012).
- ⁵ L. B. Abdalla, L. Seixas, T. M. Schmidt, R. H. Miwa, and A. Fazzio, *Phys. Rev. B* **88**, 045312 (2013).
- ⁶ T. M. Schmidt, R. H. Miwa, and A. Fazzio, *Phys. Rev. B* **84**, 245418 (2011).
- ⁷ D. Pesin and H. MacDonald, *Nature Materials* **11**, 409 (2012).
- ⁸ H. Zhang, C. X. Liu, X. L. Qi, X. Dai, Z. Fang, and S. C. Zhang, *Nature Phys.* **5**, 438 (2009).
- ⁹ Y. Xia, D. Qian, D. Hsieh, L. Wray, A. Pal, H. Lin, A. Bansil, D. Grauer, Y. S. Hor, R. J. Cava, and M. Z. Hasan, *Nature Phys.* **5**, 398 (2009).
- ¹⁰ D. Hsieh, Y. Xia, D. Qian, L. Wray, J. H. Dil, F. Meier, J. Osterwalder, L. Patthey, J. G. Checkelsky, N. P. Ong, A. V. Fedorov, H. Lin, A. Bansil, D. Grauer, Y. S. Hor, R. J. Cava, and M. Z. Hasan, *Nature Lett.* **460**, 1101 (2009).
- ¹¹ L. He, X. Kou, and K. L. Wang, *physica status solidi (RRL)* **7**, 50 (2013).
- ¹² D. Kong, W. Dang, J. J. Cha, H. Li, S. Meister, H. Peng, Z. Liu, and Y. Cui, *Nano Letters* **10**, 2245 (2010).
- ¹³ S.-K. Jerng, K. Joo, Y. Kim, S.-M. Yoon, J. H. Lee, M. Kim, J. S. Kim, E. Yoon, S.-H. Chun, and Y. S. Kim, *Nanoscale* **5**, 10618 (2013).
- ¹⁴ H. Steinberg, D. R. Gardner, Y. S. Lee, and P. Jarillo-Herrero, *Nano letters* **10**, 5032 (2010).
- ¹⁵ N. Bansal, N. Koirala, M. Brahlek, M.-G. Han, Y. Zhu, Y. Cao, J. Waugh, D. S. Dessau, and S. Oh, *Applied Physics Letters* **104**, 241606 (2014).
- ¹⁶ C.-Z. Chang, Z. Zhang, K. Li, X. Feng, J. Zhang, M. Guo, Y. Feng, J. Wang, L.-L. Wang, X.-C. Ma, *et al.*, *Nano letters* **15**, 1090 (2015).
- ¹⁷ G. Kresse and J. Furthmüller, *Phys. Rev. B* **54**, 11169 (1996).
- ¹⁸ J. P. Perdew, K. Burke, and M. Ernzerhof, *Phys. Rev. Lett.* **77**, 3865 (1996).
- ¹⁹ G. Kresse and D. Joubert, *Phys. Rev. B* **59**, 1758 (1999).
- ²⁰ H. J. Monkhorst and J. D. Pack, *Phys. Rev. B* **13**, 5188 (1976).
- ²¹ A. Tkatchenko and M. Scheffler, *Phys. Rev. Lett.* **102**, 073005 (2009).
- ²² T. Bucko, S. Lebègue, J. Hafner, and Ángyán, *Phys. Rev. B* **87**, 064110 (2013).
- ²³ H. Lind, S. Lidin, and U. Häussermann, *Phys. Rev. B* **72**, 184101 (2005).
- ²⁴ W. L. Scopel, A. J. da Silva, and A. Fazzio, *Physical Review B* **77**, 172101 (2008).
- ²⁵ R. Miwa, T. M. Schmidt, W. Scopel, and A. Fazzio, *Applied Physics Letters* **99**, 163108 (2011).
- ²⁶ M. Ishigami, J. H. Chen, W. G. Cullen, M. S. Fuhrer, and E. D. Williams, *Nano Lett.* **7**, 1643.
- ²⁷ I. S. S. de Oliveira and R. H. Miwa, *Nanotechnology* **27**, 035704 (2016).
- ²⁸ Y. Zhang, K. He, C. Chang, C. Song, L. Wang, X. Chen, J. Jia, Z. Fang, X. Dai, W. Shan, S. Shen, Q. Niu, X. Qi, S. Zhang, X. Ma, and Q. Xue, *Nat. Phys.* **6**, 584 (2010).
- ²⁹ G. Landolt, S. Schreyeck, S. V. Ereemeev, B. Slomski, S. Muff, J. Osterwalder, E. V. Chulkov, C. Gould, G. Karczewski, K. Brunner, *et al.*, *Physical Review Letters* **112**, 057601 (2014).
- ³⁰ R. F. W. Bader, *Atoms in Molecules - A Quantum Theory* (Oxford University Press, Oxford, 1990).
- ³¹ G. Henkelman, A. Arnaldsson, and H. Jónsson, *Comput. Mater. Sci.* **36**, 254 (2006).
- ³² O. V. Yazyev, J. E. Moore, and S. G. Louie, *Phys. Rev. Lett.* **105**, 266806 (2010).
- ³³ S. Kim, M. Ye, K. Kuroda, Y. Yamada, E. Krasovskii, E. Chulkov, K. Miyamoto, M. Nakatake, T. Okuda, Y. Ueda, *et al.*, *Physical Review Letters* **107**, 056803 (2011).
- ³⁴ C. Ojeda-Aristizabal, M. Fuhrer, N. Butch, J. Paglione, and I. Appelbaum, *Applied Physics Letters* **101**, 023102 (2012).
- ³⁵ Y. Liu, C. Chong, J. Jheng, S. Huang, J. Huang, Z. Li, H. Qiu, S. Huang, and V. Marchenkov, *Applied Physics Letters* **107**, 012106 (2015).
- ³⁶ By using the hybrid HSE06 approach³⁸ to the calculation of the exchange correlation energy, we find the doubly occupied defect level (V_O) at VBM+1.60 eV, where the VBM lies -8.30 eV below the vacuum level.
- ³⁷ P. Khomyakov, G. Giovannetti, P. Rusu, G. v. Brocks, J. Van den Brink, and P. Kelly, *Physical Review B* **79**, 195425 (2009).
- ³⁸ G. E. S. J. Heyd and M. Ernzerhof, *J. Chem. Phys.* **124**, 219906 (2006).